Scanning tunneling spectroscopy of Na on Cu(111)

Jörg Kliewer* and Richard Berndt†
Institut für Experimentelle und Angewandte Physik, Christian-Albrechts-Universität zu Kiel, D-24098 Kiel, Germany
(Received 22 May 2001; published 26 December 2001)

Monolayer films of Na evaporated onto Cu(111) under UHV conditions are investigated with scanning tunneling microscopy and spectroscopy (STS) at low temperature. The STS data clearly reveal a two-dimensional overlayer state of Na on Cu(111). From STS and spectroscopic imaging, the binding energies and effective masses of this state are determined for various coverages. The state is demonstrated to be affected by spatial inhomogeneities such as Cu steps or local coverage variations. Drastic bias-dependent variations of apparent step heights and tunneling barrier heights are reported and interpreted in terms of the large contributions of the overlayer state to the tunneling current.

DOI: 10.1103/PhysRevB.65.035412 PACS number(s): 73.20.−r, 73.21.−b, 68.37.Ef

I. INTRODUCTION

Alkali metal adsorption and co-adsorption on metal surfaces has attracted substantial interest in surface science, partly due to the technological relevance of these systems.[1,2] Various aspects of alkali metals adsorbed on metal surfaces have been reviewed in Refs. 3, 4, and 5. Some combinations of alkali adsorbate and metal substrate support quantum well states which represent a quasi two-dimensional electron gas (2DEG) which is confined between the vacuum barrier and the metal substrate.[6,7] In particular, data are available for the model system Na on Cu(111). Moreover, the electronic structure and dynamics of this system have recently been investigated by *ab initio* theoretical methods.[8,9]

Here we report on low-temperature ($T=5$ K) scanning tunneling microscopy (STM) and spectroscopy (STS) of room temperature grown Na layers on Cu(111). These measurements provide some information on the atomic-scale structure along with spectroscopic data. Overall, the present STM results are in agreement with electron spectroscopy data.[7,10–13] In addition, we find characteristic modifications of the electronic structure at nanoscale structures. STM turns out to be particularly useful in investigating the second Na monolayer since preparation of a perfect layer is not required. Rather, measurements may be performed on sufficiently large second layer islands.

The geometric structure of the first ML Na on Cu(111) has been investigated with low-energy electron diffraction (LEED) and STM. There is agreement that the first monolayer saturates at a coverage of 4 Na atoms per 9 Cu atoms.[12] The unit mesh is $(3/2\times 3/2)$. In this structure, the Na atom spacing is comparable to the atomic distance in bulk Na. Following Ref. 12, we define this structure as 1 monolayer (ML). As to the second Na layer, STM[14] indicates that Na grows in compact islands with a hexagonal atomic arrangement.

In discussing the electronic structure of Na on Cu(111), both the pristine Cu(111) substrate and a free Na ML in vacuum may be used as a reference. Sodium is known to significantly affect the work function $\Phi=4.85$ eV of Cu(111).[15] Φ decreases with increasing coverage down to a minimum of 2.2–2.6 eV at coverages $\Theta=0.12$–0.22.[10–13] Φ increasing again at higher Θ, a work function of 2.77–2.8 eV[10,13] is reported for the full monolayer. Similarly, the binding energy of the occupied Cu surface state shifts from ≈ -0.4 eV to lower energies and reaches the edge of the bulk states at $\Theta\approx 0.11$ where it is no longer discernible in photoelectron spectroscopy.[17,16]

Sodium also induces new unoccupied states which have been investigated with inverse photoelectron spectroscopy (IPES)[11] and two-photon photoemission (2PPE).[13] Their energy decreasing with increasing Θ, they are also observable in PES at higher coverages[16] and arrive at a binding energy of ≈ -0.1 eV at monolayer coverage. This state being located in a gap of the Cu(111) electronic structure at $\overline{\Gamma}$, it is denoted quantum well state (QWS).[7,18] According to recent first principles calculations which reproduce the Na-induced state, the local density of this state peaks on the vacuum side of the Na layer and decays rapidly on the substrate side.[9]

Below we focus on the lowest Na-induced state which is observed to cause a clear signature in scanning tunneling microscope images and spectra. Following a brief description of the experimental procedures, STS data are used to determine the binding energy of this state. We further analyze its effective mass from spectroscopic maps of scattered electron waves at defects. Next, this state is shown to have a strong impact on ''topographic'' STM images where it changes the apparent height of the second Na monolayer by some 2.5 Å. Finally, the influence of geometric nanoscale structures on this electronic state is investigated.

II. EXPERIMENTAL PROCEDURES

The experiments were performed with a custom-built ultra-high vacuum (UHV) STM operated at a temperature $T=4.6$ K.[19] Na from a thoroughly outgased commercial SAES Getters source was dosed onto a Cu(111) crystal that was previously cleaned by repeated sputter and annealing cycles. The evaporation rate was monitored with a quartz crystal microbalance. Following the preparation at room temperature the sample was transferred to the STM and cooled to $T=4.6$ K. Tunneling spectra of the differential conductance dI/dV which resembles the local density of states were recorded using a lock-in technique with modulation amplitudes ranging from 6 to 28 mV_{pp} added to the tunneling junction bias.

 ©2001 The American Physical Society

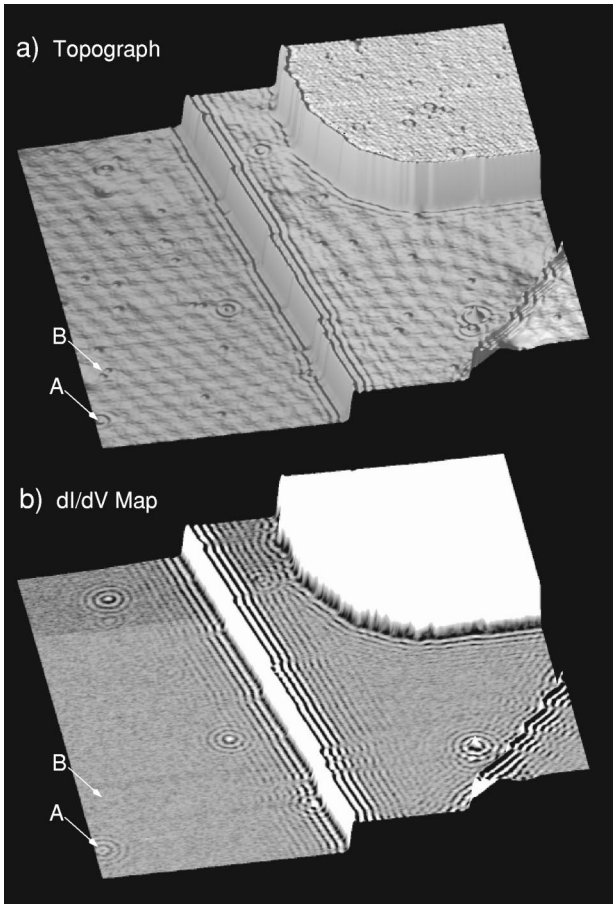

FIG. 1. Constant current topograph and spectroscopic image of first and second ML (top right island) Na film. Some protrusions (two are marked by arrows A and B) on the first ML act as scatterers for 2D electrons. ($V=102$ mV, $I=0.5$ nA, scan size 1000 $\times 1000$ Å^2).

III. BINDING ENERGIES AND EFFECTIVE MASSES

Figure 1(a) shows a constant current topograph of a Cu(111) surface at a coverage $\Theta=1.1$ ML Na. A smooth Na layer is observed in accord with previous LEED studies.[12] An analysis of atomically resolved images also confirms that Na forms a $3/2\times 3/2$ structure.[12,14] Owing to its height of 2.1 Å, the step passing approximately vertically through the image can be attributed to the Cu(111) substrate. At this step, and also at other defects, a wave pattern emerges. A map of the differential conductivity dI/dV [Fig. 1(b)] shows this wave pattern more clearly. In analogy to previous observations from Shockley surface states on noble metal surfaces,[20–22] we attribute the wave pattern to standing waves which result from scattering of a two-dimensional state at defects.

The wave pattern observed on all extended terraces is absent from the terrace in the upper right corner at the imaging conditions used suggesting that the electronic structure of this terrace is different.[23] In addition, the topographic step at the island perimeter appears to be 2.9 Å high at this tunneling voltage which is significantly larger than the value observed from Cu(111) steps (2.1 Å). We can therefore safely assign the island to the second Na monolayer (ML) on top of the Na covered Cu(111) terrace. Measurements of the apparent tunneling barrier height ϕ, which is related to the local work function, yield different values for the terrace ($\phi=2.8\pm 0.1$ eV) and the island ($\phi=2.3\pm 0.1$ eV) confirming this interpretation. Previous measurements of the work function change yielded a work function decrease of ≈ 0.4 eV when the coverage was increased from $\Theta=1$ ML to $\Theta=2$ ML in approximate agreement with our data.[12]

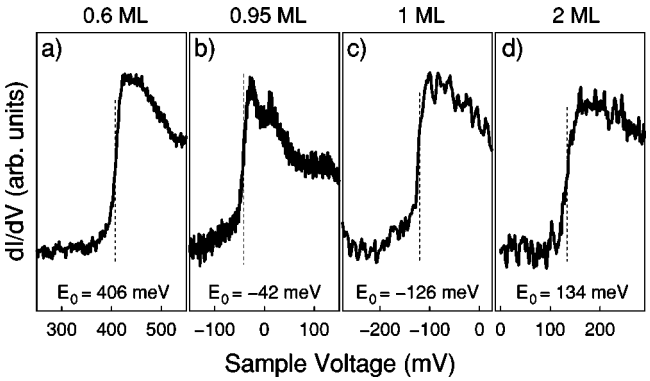

FIG. 2. dI/dV spectra Na films on Cu(111) with coverages Θ = (a) 0.6 ML, (b) 0.9 ML, (c) 1.0 ML, and (d) 2.0 ML.

We have prepared extended areas of Na layers at a number of coverages—further topographic data has been published previously[14]—and recorded their dI/dV spectra at large separations from defects. Figure 2 displays data for four different coverages. Common to all spectra is the typical signature of a two-dimensional electron gas. At a particular voltage $V_0=E_0/e$, where E_0 is the bottom of the two-dimensional band, dI/dV exhibits a sharp rise. While V_0 defined as the midpoint of the rise is independent of the tip status, the decrease of dI/dV at higher voltages does depend to some extent on the particular tip. The binding energies determined from Fig. 2 and many other measurements using various tips are compiled in Table I. As expected on the basis of previous electron spectroscopic results, the STM data

TABLE I. Binding energy E_0 (in meV) and effective mass m^* (in units of the electron mass) of the Na induced state from STM, PES, or IPES experiments and density-functional (DFT) calculations.

Coverage	E_0 this work	m^* this work	E_0 (I)PES	E_0 DFT	m^* (I)PES	m^* DFT
0.6	408		400[a]	450[c]	1.22[b]	0.96[c]
			560[b]			
0.9	-44	0.6 ± 0.02	-45[e]			
1.0	-127	0.7 ± 0.04	-110[d]	-60[c]	1.3[d]	0.78[c]
			-97[e]		0.5[e]	
2.0	134	1.06 ± 0.06	≈ 100[e]			

[a]Reference 27.
[b]Parabolic fit to data from Ref. 27 quoted after Ref. 8.
[c]Reference 9.
[d]Reference 13.
[e]Reference 18.

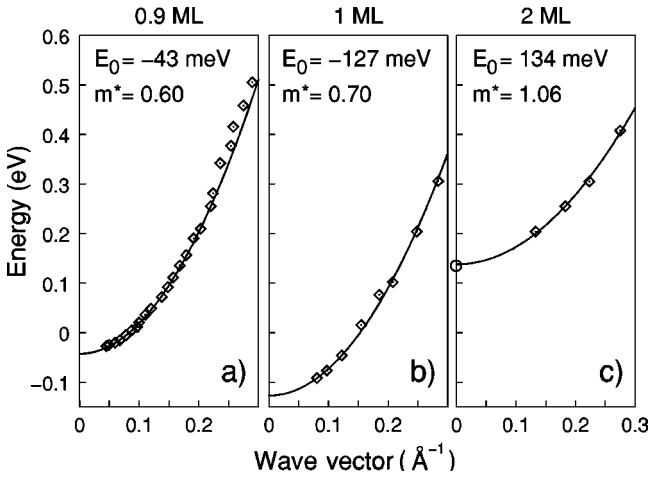

FIG. 3. Dispersion relation $E(K)$ of the lowest QWS for coverages Θ (a) 0.9 ML, (b) 1.0 ML, and (c) 2.0 ML. Diamonds represent experimental data. Solid lines are the result of parabolic fits with E_0 and m^* as free parameters. In the case of $\Theta=2$ ML, E_0 was determined from tunneling spectroscopy (open circle in c) leaving only m^* as a free parameter.

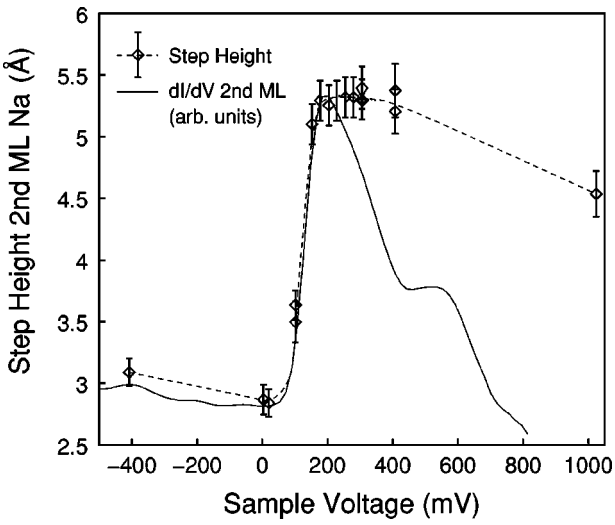

FIG. 4. Step height of second ML Na island as a function of sample voltage (diamonds, including error bars, the dashed line serves to guide the eye) and dI/dV spectrum of the second ML (solid line).

show a rapid variation of the binding energy of the Na-induced state with coverage. The small differences between electron spectroscopy and STM are most likely due to differences of the coverage calibration. Averaging over spatial variations of E_0 owing to coverage fluctuations may also play a role in (I)PES.

In dI/dV spectra of the first monolayer, in addition to the QWS-related rise at -126 meV, three further features have been reproducibly observed at $\approx -900, -600$, and -400 meV.[24] While at present no assignment of these structures can be made, we note that these features are absent from spectra recorded close to steps which indicates that they are not caused by the tip electronic structure. Moreover, spectra of the second ML exhibit this structure, too, albeit at strongly reduced intensities. A possible explanation of these features may be Cu-derived states. A recent density-functional calculation of Na on Al(111) reported such states at energies below the Na-induced band.[25]

Scattering of the 2D Na states at defects gives rise to electron standing wave patterns (Fig. 1). These patterns and their voltage dependence are detectable over an extended range of bias voltages and, therefore, enable a measurement of the dispersion of the 2D states. We applied the technique of Li *et al.*[26] to extract $E(k)$ from the standing wave patterns near straight steps. Briefly, the analysis is based on fitting line scans of constant current topographic and dI/dV images perpendicular to straight steps with a model calculation of the tunneling current. Figure 3 summarizes our results. In the three cases investigated—0.9, 1, and 2 ML—it is possible to fit the experimental dispersion by parabolic relations which yield the effective masses indicated in Table I.[27] We note that the data derived from the standing wave patterns yield binding energies E_0 which are consistent with those obtained from dI/dV spectroscopy. Despite the good agreement between the present and previous data in terms of E_0, the effective mass of the Na QWS at $\Theta=1$ ML differs considerably from previous results. From IPES and 2PPE values of 1.3 and 0.5 were determined whereas the STM data yield 0.7. Given the deviation between experiments and DFT calculations with respect to E_0 the good agreement of the DFT effective mass of 0.78 with the present experimental data may be fortuitous.

IV. STEP HEIGHTS

During the present experiments on Na films, the height of the second monolayer was observed to depend strongly on the sample voltage which is rather unusual for metallic systems (Fig. 4). While the step height is around 3 Å at negative sample bias, at $V\approx 100$ mV a sharp increase of the step height by up to 2.5 Å occurs, leading to an apparent step height of ≈ 5.5 Å. At higher V, the step height appears to decrease to ≈ 4.5 Å. It should be noted that we observed quantitatively different height variations with different tips while the qualitative characteristics were always observed. The smallest step height of ≈ 3 Å is comparable to the smallest interlayer spacing for bulk Na (3.0 Å). To interpret the voltage dependent increase of the apparent height a dI/dV spectrum on top of a second ML island is displayed in Fig. 4 (solid line). The increase in step height strongly correlates with the LDOS of the unoccupied QWS at $E_0=134$ meV. This correlation is not unexpected. When the unoccupied second ML Na QWS is not accessible for tunneling, the current is due to bulk electrons alone. For $V\geqslant 134$ mV, however, an additional channel for tunneling electrons opens up and the resulting increased conductance causes the feedback loop to retract the tip by up to 2.5 Å to maintain a constant current.

The observations from steps and dI/dV spectra demonstrate that the contribution of the QWS to the tunneling current can be switched on or off by applying suitable bias voltages. This possibility enables a degree of selectivity in

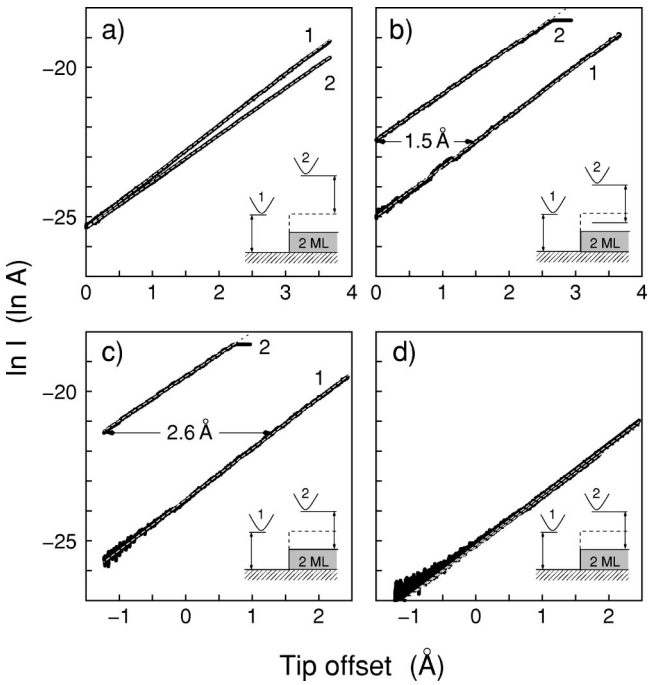

FIG. 5. Logarithmic $I(z)$ data of the first and second ML Na film. Negative values of z correspond to decreased tip-sample distances. The insets schematically show the measurement geometry: The tip is either placed above the first ML (1) or the second ML (2). The tip sample distance prior to opening the feedback loop depends on the bias voltage V_f. Above the first ML (tip position 1), both bulk and Na overlayer state electrons contribute to the tunneling current. Above the second ML (tip position 2) the situation is different: In (a) the voltage is $V_f=300$ mV, i.e., both bulk and second ML QWS electrons contribute to the tunneling current, whereas in (c) and (d) ($V_f=20$ mV and $V_f=4$ mV) the voltage V_f is adjusted such that only bulk electrons contribute. Part (b) ($V_f=100$ mV) represents an intermediate case.

measurements of the tunneling barrier height $\phi(\mathrm{eV}) = 0.952[d \ln I(\mathrm{A})/dz(\mathrm{Å})]^2$. The work function of the sample being significantly lower than that of the tungsten tip, ϕ is related to the local sample work function.[28] Figure 5 summarizes measurements of ϕ from the first (marked "1") and second ML (marked "2") under various conditions. Before interrupting the STM feedback loop, the tip-sample separation was defined by the current set-point (either 0.1 nA or 0.01 nA) and the voltage V_f. During the $I(z)$ measurement (feedback loop open) a voltage V_m was used. Using both $V_f=300$ mV and $V_m=300$ mV [Fig. 5(a)] leads to exponential current-distance curves from the first and second ML. The resulting apparent tunneling barrier heights are $\phi_1 = 2.8$ eV and $\phi_2=2.3$ eV. The 20% reduction of the barrier height on the second ML is consistent with previous work function measurements.[10,13,12] Using feedback at energies below the QWS [$V_f=100$ mV and $V_f=20$ mV, Figs. 5(b) and 5(c)] and recording $I(z)$ at $V_m=300$ mV above the QWS yields virtually unchanged barrier heights $\phi_1 = 2.7$ eV, $\phi_2=2.3$ eV. Neglecting for a moment the different slopes of the $I(z)$ data of the first and second ML, we observe that by shifting the 1st layer data by ≈ 1.5 Å and ≈ 2.6 Å in Figs. 5(b) and 5(c), respectively, the second layer $I(z)$ is obtained. These offsets do agree with the step heights from Fig. 4.

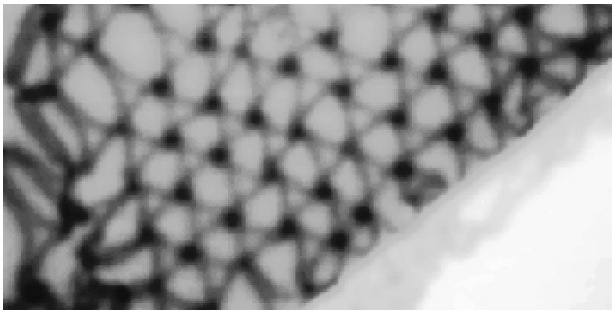

FIG. 6. Constant current image of Na/Cu(111), $\Theta=0.6$ ML, scan size 630×290 Å^2, $V=400$ mV, $I=0.2$ nA.

Finally, to eliminate the QWS contribution to the current, Fig. 5(d) was recorded with $V_f=V_m=4$ mV. As a result, no difference in slope of the $I(z)$ data from the first and second ML is observed with 2.61 eV$=\phi_1\approx\phi_2=2.69$ eV. Both values are close to the first ML value reported above. The data from Figs. 4 and 5 highlight the importance of the QWS of the second ML for the tunneling current. "Switching on" the QWS in going from Fig. 5(d) to Fig. 5(c) results in a QWS-related increase of the current by a factor of ≈ 55. The QWS also has a strong impact on the apparent barrier height.

V. SPATIAL INHOMOGENEITIES

A unique opportunity of STS is the ability to image the morphology of surfaces areas selected for spectroscopic measurement. In the case of Na layers we observed spatial variations of the geometric structure which also involve varying electronic structure. A particularly intriguing case are films with $\Theta\approx 0.6$ ML (Fig. 6). At this coverage, we observe partially ordered networks of trenches (width ≈ 30 Å) separating "islands" with a typical diameters of ≈ 40 Å. We have attributed these trenches to locally decreased Na density which separate p(2×2) areas.[14] Figure 7 displays a number of characteristic spectra. Spectrum F which was recorded from a flat terrace and exhibits the typical shape of a surface state band with a sharp rise at the band

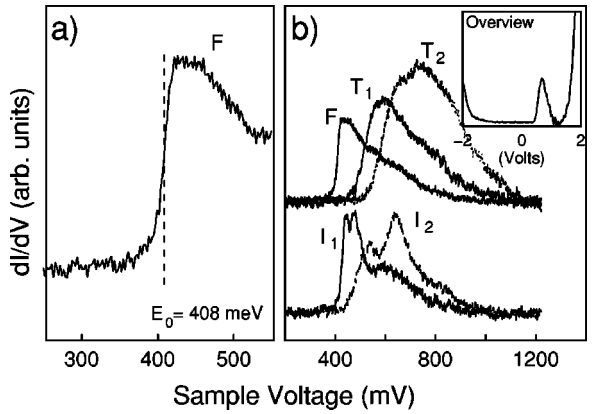

FIG. 7. Characteristic dI/dV spectra recorded at different locations above 0.6 ML Na films.

bottom and a decay of dI/dV toward higher voltages. The spectra from p(2×2) islands (I_1, I_2) show extra structure at higher energies which is consistent with the formation of confined electronic states in these islands. The confinement apparently is induced by the lower coverage trenches. Typically, spectra from these trenches (spectra T_1, T_2) show a broadened and strongly shifted band edge.

Electronic differences between trenches and islands also occur in measurements of the apparent tunneling barrier height. We find $\phi(F)=2.5$ eV, $\phi(T_1)=2.9$ eV, $\phi(T_2)=3.0$ eV. Previous measurements of the work function change at room temperature[12] showed that a uniform decrease of the work function for Θ up to 0.5 ML suggesting that the trenches do indeed correspond to regions with low Na coverage. Consistent with this observation, E_0 measured at the trenches yields larger values than observed on terraces as expected from electron spectroscopy data.[17,18]

At coverages above 1 ML, homogeneous second ML islands were observed. These islands were found to clearly confine the QWS of the second ML. Figure 8 shows a series of dI/dV maps from an island (area $\approx 200\times200$ Å^2) which were recorded at various energies above the band minimum of the QWS. As expected, similar to previous observations from noble metal islands,[29–31] an evolution of dI/dV (which resembles the local density of states) from a single maximum at low bias to more complex patterns is observed. The unusual appearance of the island in the constant current image is caused by the large contribution of the QWS to the tunneling current.

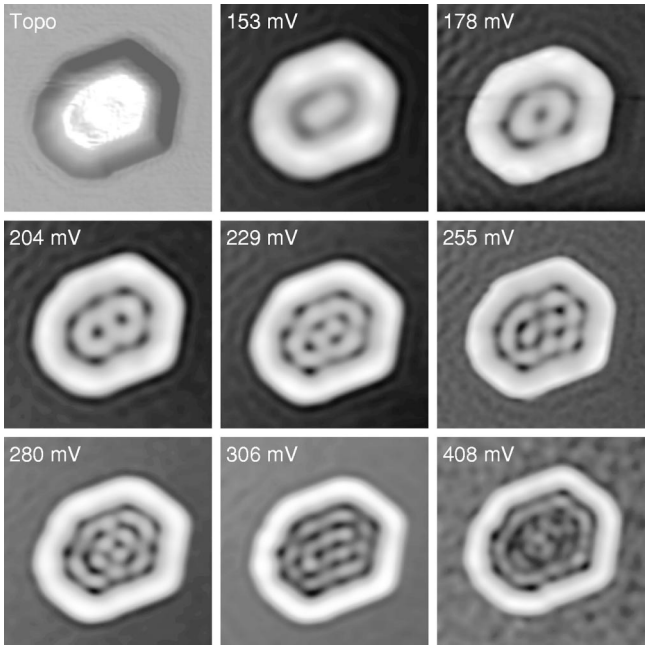

FIG. 8. Topographic scan (top left image) and dI/dV maps of a second layer Na island recorded at the voltages indicated. Scan area 200×200 Å^2.

VI. SUMMARY

We have investigated electronic states of Na-covered ($\Theta=0.6$–2 ML) Cu(111) surfaces with low-temperature STM. For the lowest Na-induced quantum well state binding energies and effective masses are determined which reasonably agree with previous electron spectroscopy data and density-functional calculations. The local density of states of the QWS being large above the crystal surface this state contributes strongly to the tunneling current when it is energetically accessible. As a result, apparent step heights of Na layers and tunneling barrier heights vary drastically with the tip-sample voltage. The QWS is affected by spatial inhomogeneities as demonstrated for monoatomic steps of the Cu substrate which cause clear scattering patterns. Moreover, at submonolayer coverage, networks of apparent depressions are observed in STM images which we have tentatively attributed to locally lowered Na coverage on the basis of work function data. Spectra from these trenches clearly differ from spectra of homogeneous areas. Finally, for second ML islands, confined electronic states have been observed.

ACKNOWLEDGMENTS

We are delighted to thank J. Carlsson, R. Diehl, B. Hellsing, H. Over, and L. Walldén for discussions. Financial support by the Deutsche Forschungsgemeinschaft and the Forschungsverbund Nanowissenschaften NRW is gratefully acknowledged.

*Present address: Infineon Technologies AG, Postfach 800949, D–81609 München.

†Electronic address: berndt@physik.uni-kiel.de

[1] E. G. Bauer, in *The Chemical Physics of Solid Surfaces and Heterogeneous Catalysis*, Vol. 3B, edited by D. A. King and D. P. Woodruff (Elsevier, New York, 1983).

[2] A. M. Bradshaw, H. P. Bonzel, and G. Ertl, *Physics and Chemistry of Alkali Metal Adsorption* (Elsevier, Amsterdam, 1989).

[3] R. D. Diehl and R. McGrath, Surf. Sci. Rep. **23**, 43 (1996).

[4] C. Stampfl and M. Scheffler, Surf. Rev. Lett. **2**, 317 (1995).

[5] H. Tochihara and S. Mizuno, Prog. Surf. Sci. **48**, 75 (1998).

[6] S.-Å. Lindgren and L. Walldén, Solid State Commun. **34**, 671 (1980).

[7] S.-Å. Lindgren and L. Walldén, Phys. Rev. Lett. **59**, 3003 (1987).

[8] B. Hellsing, J. Carlsson, L. Walldén, and S.-Å. Lindgren, Phys. Rev. B **61**, 2343 (2000).

[9] J. M. Carlsson and B. Hellsing, Phys. Rev. B **61**, 13973 (2000).

[10] S.-Å. Lindgren and L. Walldén, Phys. Rev. B **22**, 5967 (1989).

[11] R. Dudde and B. Reihl, Phys. Rev. **44**, 1198 (1991).

[12] D. Tang, D. McIlroy, X. Shi, C. Su, and D. Heskett, Surf. Sci. Lett. **255**, L497 (1991).

[13] N. Fischer, S. Schuppler, R. Fischer, Th. Fauster, and W. Steinmann, Phys. Rev. B **43**, 14722 (1991).

[14] J. Kliewer and R. Berndt, Surf. Sci. **477**, 250 (2001).

[15] P. O. Gartland and B. J. Slagsvold, Phys. Rev. B **12**, 4047 (1975).

[16] S.-Å. Lindgren and L. Walldén, Phys. Rev. B **38**, 3060 (1988).

[17] N. Fischer, S. Schuppler, Th. Fauster, and W. Steinmann, Surf. Sci. **314**, 89 (1994).

[18] A. Carlsson, B. Hellsing, S.-Å. Lindgren, and L. Walldén, Phys. Rev. B **56**, 1593 (1997).
[19] J. Kliewer, Ph. D. thesis, RWTH Aachen, D-52056 Aachen, Germany (2000).
[20] L. C. Davis, M. P. Everson, R. C. Jaklevic, and W. Shen, Phys. Rev. B **43**, 3821 (1991).
[21] Y. Hasegawa and Ph. Avouris, Phys. Rev. Lett. **71**, 1071 (1993).
[22] M. F. Crommie, C. P. Lutz, and D. M. Eigler, Science **262**, 218 (1993).
[23] At $V=102$ mV, the two-dimensional state of the first ML is accessible to tunneling electrons. Their energy is below the band minimum of the second ML state: E_0 (first ML) $=-126$ meV$<E<E_0$(second ML)$=134$ meV.
[24] J. Kliewer and R. Berndt, Appl. Phys. A: Mater. Sci. Process. **72**, S155 (2001).
[25] C. Stampfl, K. Kambe, R. Fasel, P. Aebi, and M. Scheffler, Phys. Rev. B **57**, 15251 (1998).
[26] J. Li, W.-D. Schneider, and R. Berndt, Phys. Rev. B **56**, 7656 (1997).
[27] R. Dudde and B. Reihl, Surf. Sci. **287**, 614 (1993).
[28] N. D. Lang, Phys. Rev. B **34**, 5947 (1986).
[29] Ph. Avouris and I.-W. Lyo, Science **264**, 942 (1994).
[30] J. Li, W.-D. Schneider, R. Berndt, and S. Crampin, Phys. Rev. Lett. **80**, 3332 (1998).
[31] J. Li, W.-D. Schneider, R. Berndt, and S. Crampin, Surf. Sci. **422**, 95 (1999).